Gait & Posture 31 (2010) 57–63

Contents lists available at ScienceDirect

Gait & Posture

journal homepage: www.elsevier.com/locate/gaitpost

Implications of using hierarchical and six degree-of-freedom models for normal gait analyses

Frank L. Buczek [a,c,*], Michael J. Rainbow [b], Kevin M. Cooney [c], Matthew R. Walker [d], James O. Sanders [e]

[a] National Institute for Occupational Safety & Health, Morgantown, WV, USA
[b] Brown University, Providence, RI, USA
[c] Shriners Hospitals for Children, Erie, PA, USA
[d] York University, Toronto, Ontario, Canada
[e] University of Rochester, Rochester, NY, USA

ARTICLE INFO

Article history:
Received 26 February 2009
Received in revised form 21 August 2009
Accepted 31 August 2009

Keywords:
Six degree-of-freedom
Conventional gait model
Helen Hayes
Hierarchical
Normal
Human

ABSTRACT

Hierarchical biomechanical models (conventional gait model, CGM) are attractive because of simple data collection demands, yet they are susceptible to errors that are theoretically better controlled using six degree-of-freedom models that track body segments independently (OPT1). We wished to compare gait variables obtained with these models. Twenty-five normal children walked while wearing a hybrid marker configuration, permitting identical strides to be analyzed using CGM and OPT1. Kinematics and ground reaction forces were obtained using a common motion capture system. CGM and OPT1 were implemented in Visual3D software, where inverse dynamics provided 20 clinically relevant gait variables (joint angles, moments and powers). These were compared between models using dependent *t*-tests (Bonferroni-adjusted alpha of 0.0025), and ensemble averages. We hypothesized that OPT1 would provide data similar to CGM in the sagittal plane, and different from CGM in coronal and transverse planes. Six variables were significantly different in the sagittal plane, suggesting that CGM produced a more extended lower extremity; this was explained by a posterior bias to the lateral knee marker during knee flexion, as a result of skin movement artifact. No significant differences were found in coronal plane variables. Four variables were significantly different in the transverse plane. Ensemble averages were comparable between models. For normal children, biomechanical interpretations based upon these tested variables are unlikely to change due to independent segment tracking alone (CGM vs. OPT1). Additional differences may appear due to pathology, and when segment reference frames are changed from those used in CGM to reflect individual anatomy.

1. Introduction

Hierarchical biomechanical models are attractive because of their simple marker configurations and data collection demands, yet they are susceptible to errors that are theoretically better controlled using models that treat body segments independently. The conventional gait model (CGM) is widely used today for clinical gait analyses. It was developed decades ago, with slight variations among sites, using a hierarchical structure to overcome equipment limitations of the time period [1,2]. In particular, video-based motion capture systems were in their infancy, and required time-consuming manual intervention for marker identification and tracking. To limit this labor-intensive task, three-dimensional analyses were achieved using a biomechanical model that required the fewest possible markers. Although this was an ingenious way to practically implement an important clinical service, several undesirable mathematical consequences resulted: (a) there was incomplete control in identifying joint centers and axes of rotation, (b) body segments were not tracked independently, allowing errors to cascade from the pelvis, through the thigh, shank, and foot segments, (c) the foot was modeled using only two rotational degrees-of-freedom, and (d) the lack of redundant markers prevented the use of least squares techniques to control for measurement error (see Online Supplemental Information for a more detailed discussion). More recently, global optimization techniques have been used to drive CGM output variables (e.g., joint kinematics) toward expected outcomes [3–5]. Proponents of global optimization believe it adequately addresses shortcomings in CGM, however, the kinematic solution to which the optimization is driven reflects normal joint anatomy and function, and may not be suitable for joints disrupted by pathology. Other solutions avoid

* Corresponding author at: NIOSH/HELD/ECTB, 1095 Willowdale Road, MS2027, Morgantown, WV 26505, USA. Tel.: +1 304 285 5966; fax: +1 304 285 6265.
E-mail address: fbuczek@cdc.gov (F.L. Buczek).

0966-6362/$ – see front matter © 2009 Elsevier B.V. All rights reserved.
doi:10.1016/j.gaitpost.2009.08.245

CGM altogether, and do not presuppose a known kinematic outcome [6]. A least squares, six degree-of-freedom (6DoF) approach uses an over-determined set of physical markers to independently track individual segments while accounting for measurement error [7–9]. Such an approach is theoretically more robust to unexpected anatomical variations that result from pathology. Least squares, 6DoF kinematics provide more complete input for induced acceleration analyses [10], may eliminate the need for more demanding least squares kinetics in forward dynamic simulations [11], and may facilitate subject-specific muscle models [5].

A need exists for comparisons, and accuracy assessments, of gait analysis variables calculated using CGM and various 6DoF modeling techniques. Of particular interest are models that may be termed CGM, OPT1 (CGM joint centers and local reference frames (LRFs), with least squares, 6DoF tracking), and OPT2 (joint centers and LRFs based upon cadaver and medical imaging studies, with least squares, 6DoF tracking). As a first step in meeting this need, this study compares typical gait analysis variables across CGM and OPT1 models for normal children, i.e., we explore only the effects of 6DoF tracking techniques while using joint centers and LRFs defined by CGM. We hypothesized that OPT1 would provide clinically relevant gait data similar to CGM in the sagittal plane, and different from CGM in both coronal and transverse planes.

2. Methods

Twenty-five normal volunteers (15 male, 10 female, mean age 11.0 years (SD 3.1), body mass 38.8 kg (17.2), height 1.454 m (0.204)) were admitted to the study following informed consent approved by our local human subjects committee. None had previous injury to the lower extremities. Upon arrival, subjects donned athletic shorts (and tops for females) provided by the investigators, and several anthropometric measurements were taken for later use in biomechanical modeling (e.g., body mass, height, distance across bilateral anterior-superior iliac spines (ASIS), bilateral leg length measured from ASIS to ipsilateral medial malleolus, and bilateral tibial torsion [12]). Surface electromyography (EMG) electrodes (not relevant for the current study) were applied to the bilateral rectus femoris, vastus lateralis, medial hamstrings, anterior tibialis, and gastrocnemius muscles, and connected to a back-pack fastened to a neoprene vest. Landmark and tracking markers were applied (Fig. 1, Table 1), and subjects were asked to stand quietly for a static calibration. After landmark markers were removed, subjects walked at a self-selected pace along a straight path, approximately 10 m in length, in view of observational and motion capture cameras. Their starting point was adjusted to facilitate clean contacts with at least one of three force plates barely discernible in the floor. After five clean force plate contacts were obtained bilaterally, testing was concluded; this typically required about 15 walking trials.

Two biomechanical models were created in Visual3D (C-Motion, Inc., Rockville MD, USA). CGM was implemented using the Helen Hayes option for the lower extremities and pelvis (Fig. 1, Table 1); OPT1 began with CGM joint centers and LRFs, but tracked all body segments using a minimum of four physical markers. In both models, a static subject calibration was used to define these joint centers and LRFs, rather than computing these for each dynamic frame as was done in some CGM implementations (e.g., Vicon Clinical Manager, Oxford Metrics Group, Oxford, England, UK). This hybrid marker set allowed a single stride to be analyzed for each subject, using both CGM and OPT1 models. Although not used in the current study, upper body kinematic data were

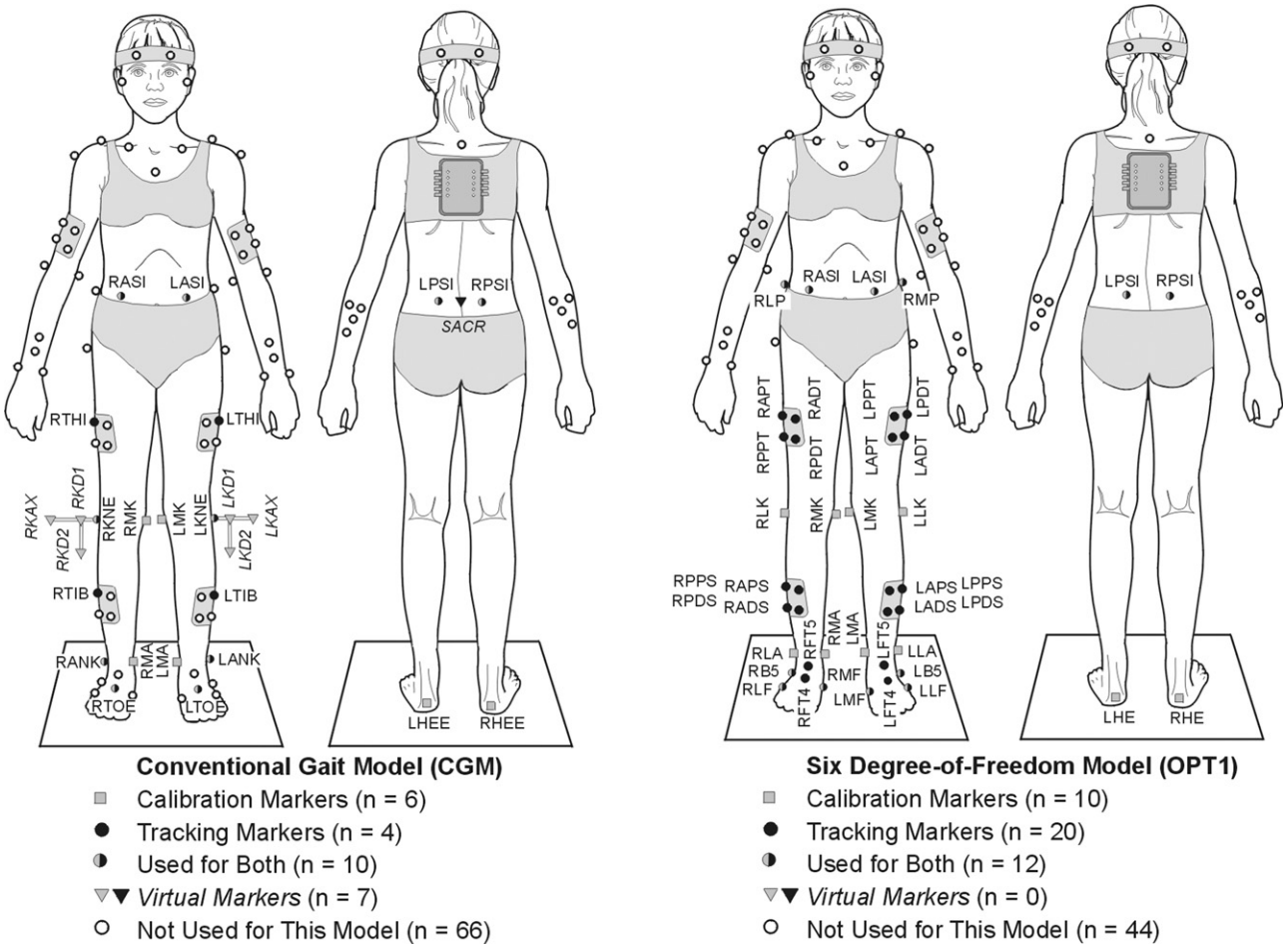

Fig. 1. Hybrid marker configuration. Although a full-body marker configuration was used, only the pelvis and lower extremities were analyzed in this study. This hybrid configuration allowed post-processing of the same stride using both CGM and OPT1. See Table 1 for marker descriptions. CGM was implemented per Kadaba et al. [1] and Davis et al. [2]. A virtual knee alignment device (KAD) was created based upon physical markers on the medial and lateral femoral epicondyles. A virtual sacral marker was created as the mid-point between markers on the bilateral posterior-superior iliac spines. One marker from each thigh and shank cluster was used as a surrogate for mid-segment wands. OPT1 used joint centers and local reference frames identical to those in CGM, but all body segments were tracked independently using a minimum of four physical markers.

Table 1
Marker descriptions for conventional (CGM) and six degree-of-freedom (OPT1) models.

CGM	OPT1	Description
		Pelvis
L/RASI	L/RASI	(Left and right) anterior-superior iliac spine
L/RPSI	L/RPSI	Posterior-superior iliac spine
	RLP	Right iliac crest
	RMP	Left iliac crest
SACR		Sacrum
		Thigh
L/RTHI	L/RPPT	Thigh (posterior proximal thigh)
	L/RPDT	Posterior distal thigh
	L/RADT	Anterior distal thigh
	L/RAPT	Anterior proximal thigh
L/RKNE	L/RLK	Lateral femoral epicondyle
L/RMK	L/RMK	Medial femoral epicondyle
L/RKD1		Knee alignment device—arm 1
L/RKD2		Knee alignment device—arm 2
L/RKAX		Knee alignment device—axis
		Shank
L/RTIB	L/RPPS	Tibia (posterior proximal shank)
	L/RPDS	Posterior distal shank
	L/RADS	Anterior distal shank
	L/RAPS	Anterior proximal shank
L/RANK	L/RLA	Lateral malleolus
L/RMA	L/RMA	Medial malleolus
		Foot
L/RTOE	L/RFT4	Midshaft, between second and third metatarsals
L/RHEE	L/RHE	Most posterior point on calcaneus
	L/RB5	Base of fifth metatarsal
	L/RLF	Head of fifth metatarsal
	L/RMF	Head of first metatarsal
	L/RFT5	More proximal than L/RFT4

also collected. Dynamic skeletal graphics, created in Visual3D and driven by subject kinematics, were used to assist with the interpretation of results.

In general, our anatomically defined LRFs provided the pose of adjacent body segments such that no offsets were needed to produce commonly accepted joint kinematics. An exception occurred for the foot segment, where the lack of an offset resulted in a plantarflexion bias at the ankle complex. We chose to accept this limitation because of difficulties in deriving a single offset algorithm that would be appropriate for both CGM and OPT1. These difficulties arose because, in clinical practice, model specific rather than hybrid markers would be available. Using different model specific offsets for CGM and OPT1 would have violated our goal of using identical processing apart from tracking methods (hierarchical vs. 6DoF). Because our LRFs for the foot and shank were identical for CGM and OPT1, our comparisons between these models would still be valid, despite a bias toward plantarflexion when compared with the literature.

Retro-reflective landmark and tracking markers were 6 mm in diameter. The latter were fixed to thermoplastic shells held in place by circumferential elastic wrap; the undersides of these shells were covered in Dycem (Dycem Limited, Warwick RI, USA) to limit slippage against the skin that could deleteriously affect calculated joint translations. Marker trajectories were collected at 120 Hz using a 10-camera Vicon 612 system (Oxford Metrics Group, Oxford, England, UK). Calibration residuals were on the order of 1 mm, for a control volume approximately 2 m wide, 4 m long, and 2 m high. Interpolation and low-pass filtering (6 Hz cutoff) were performed in Visual3D. Ground reaction forces were collected at 1560 Hz using three AMTI OR6-7 force plates (Advanced Mechanical Technology, Inc., Watertown, MA, USA), and were analog low-pass filtered at 1050 Hz. EMG data (not used in this study) were collected using an MA-300 system (Motion Lab Systems, Baton Rouge, LA, USA), tethered to the back-pack worn by the subjects.

Dependent *t*-tests (Statistica, StatSoft, Tulsa, OK, USA) detected differences in 20 key, functionally-grouped, gait analysis variables calculated in Visual3D (Table 2), using a Bonferroni-adjusted alpha of 0.0025 for any single comparison (i.e., 0.05/20). These variables were deemed important for the majority of clinical gait analyses performed in our laboratory. To help illustrate overall differences between models, ensemble averages were calculated for joint angles, moments, and powers, in locally defined sagittal, coronal, and transverse planes.

3. Results

Our hypotheses were partially supported. Six of nine variables were significantly different in the sagittal plane (Table 2, Fig. 2).

Table 2
Statistical comparison of key gait analysis variables across models ($n = 25$).

Variable		CGM		OPT1		*p* value
		Mean	St. dev	Mean	St. dev	
Iliopsoas tightness (sagittal)						
1	Maximum hip extension in late stance (°)	−8.515	5.884	−6.642	5.522	0.0000*
2	Maximum hip flexion moment in late stance (N m/kg)	−0.6552	0.1619	−0.6277	0.1489	0.0269
3	Maximum hip flexion power absorption in late stance (W/kg)	−0.7469	0.3769	−0.6416	0.2992	0.0007*
Hamstring tightness (sagittal)						
4	Maximum knee extension in late swing (°)	−1.715	4.102	−0.1183	4.773	0.0003*
5	Maximum knee flexion moment in late swing (N m/kg)	−0.2096	0.0619	−0.2031	0.0622	0.0137
6	Maximum knee flexion power absorption in late swing (W/kg)	−0.8849	0.3039	−0.8767	0.3002	0.5296
Ankle propulsion (sagittal)						
7	Maximum ankle plantarflexion at push-off (°)	−39.00	6.304	−42.29	8.411	0.0005*
8	Maximum ankle plantarflexion moment (N m/kg)	1.296	0.1988	1.329	0.2034	0.0000*
9	Maximum ankle plantarflexion power generation (W/kg)	2.980	1.028	3.473	1.163	0.0000*
Gluteus medius weakness (coronal)						
10	Maximum hip adduction in early stance (°)	5.800	3.788	5.567	3.950	0.1995
11	Maximum hip abduction moment in early stance (N m/kg)	0.5316	0.1277	0.5185	0.1379	0.1164
12	Maximum hip abduction power absorption early stance (W/kg)	−0.2091	0.1155	−0.2786	0.1774	0.0040
Knee loading (coronal)						
13	Maximum knee adduction moment at initial contact (N m/kg)	−0.0956	0.0643	−0.1022	0.0697	0.1738
14	Maximum knee abduction moment in early stance (N m/kg)	0.2543	0.1158	0.2330	0.1234	0.0108
Lesser known biomechanics (transverse)						
15	Mean hip int/ext rotation across gait cycle (°)	−3.034	7.607	−5.224	7.249	0.0022*
16	Mean knee int/ext rotation across gait cycle (°)	−5.846	8.319	−8.660	8.371	0.0000*
17	Mean ankle int/ext rotation across gait cycle (°)	−3.316	5.626	1.937	5.741	0.0000*
18	Maximum hip external rotation moment early stance (N m/kg)	0.1701	0.0736	0.1652	0.0761	0.0825
19	Maximum knee external rotation moment late stance (N m/kg)	0.1120	0.0402	0.1001	0.0441	0.0000*
20	Maximum knee internal rotation moment early stance (N m/kg)	−0.0675	0.0359	−0.0739	0.0361	0.0351

Notes: Joint moments are intrinsic and reported with respect to the local reference frame in the proximal segment. Kinetic data (moments and powers) are normalized by body mass.

* Significant at $p < 0.0025$.

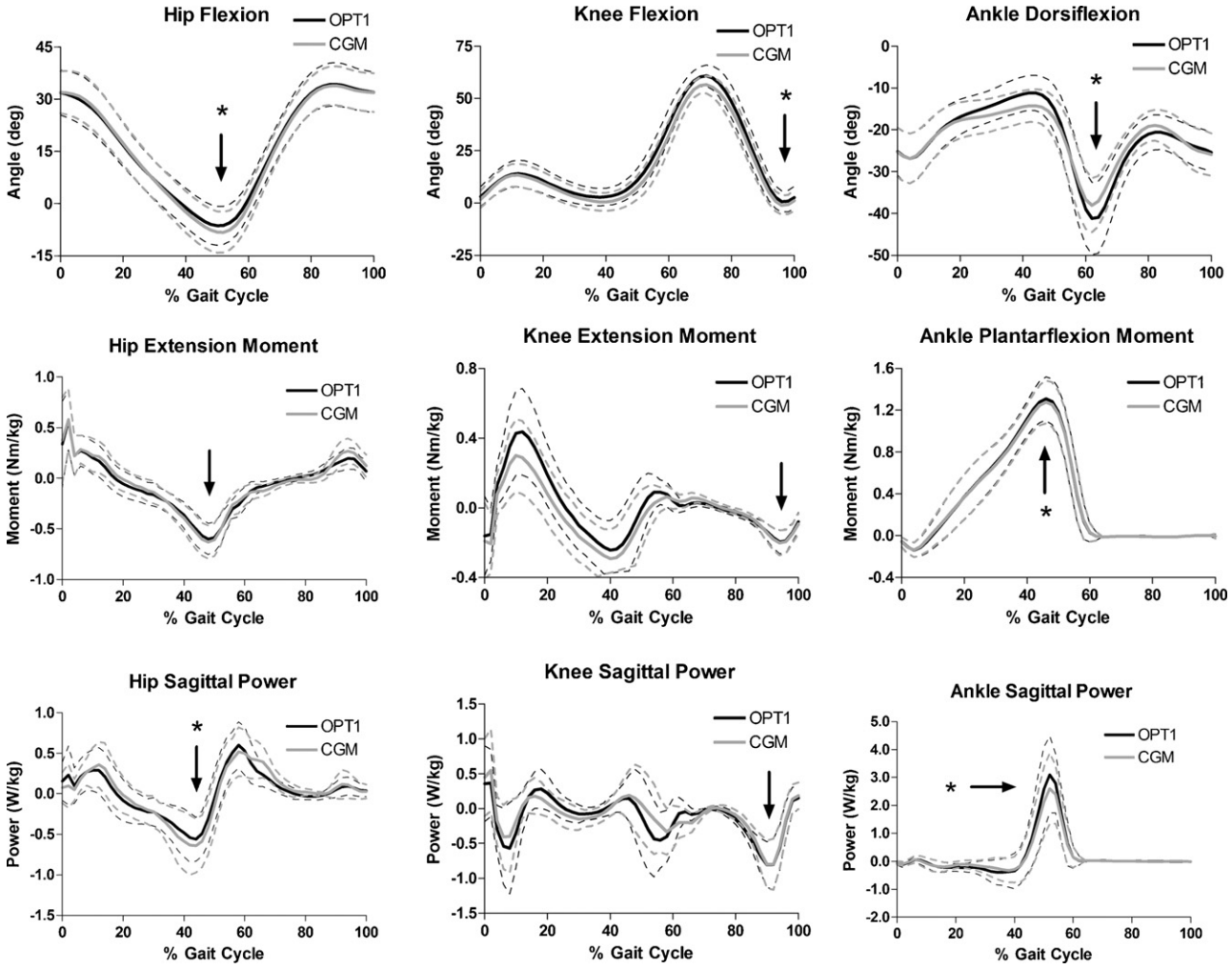

Fig. 2. Sagittal plane ensemble averages for 25 normal children. Black arrows indicate where CGM (solid gray) and OPT1 (solid black) were compared statistically with dependent *t*-tests; asterisks indicate significant differences ($p < 0.0025$); dashed lines indicate ±one standard deviation. *Note*: Because of difficulties in deriving an offset algorithm for the foot local reference frame that would be appropriate for both CGM and OPT1, we applied no offset, and there is a resulting bias toward plantarflexion at the ankle complex. See text for details.

Individual sagittal plane results at the hip, knee, and ankle suggested that CGM systematically produced a more extended lower extremity that might be explained by a posterior bias to the lateral knee marker during knee flexion. This was confirmed via reference to dynamic skeletal graphics for a representative subject (see Online Supplemental Information). No significant differences were found in five coronal plane variables (Table 2, Fig. 3). Four of six variables were significantly different in the transverse plane, and these were appreciated graphically (Table 2, Fig. 4).

4. Discussion

We sought to determine the implications of using hierarchical (CGM) and 6DoF (OPT1) gait models, focusing on the effects of different tracking techniques while using joint centers and LRFs defined by CGM. We found qualitative differences in ensemble averages for joint angles, moments, and powers, and statistically significant differences for several key kinematic and kinetic gait variables. While many of these differences were subtle and unlikely to affect clinical interpretations of these normal data, others were more substantial and deserving of further investigation. To put these differences in perspective, we compared our results with those obtained in studies using CGM with skin mounted markers, and in studies using various *in vitro* and *in vivo* models free from skin movement artifact.

4.1. Studies using CGM with skin mounted markers

Ensemble averages for sagittal plane joint angles, moments, and powers (Fig. 2) were comparable between CGM and OPT1, and were very similar to those reported by others using CGM [13–15], with one caveat. Although our ankle dorsiflexion data were not corrected for a standing offset, they were otherwise of similar shape and range-of-motion. Significant differences between sagittal plane gait variables (Table 2) were not appreciated graphically for two, largely statistical, reasons. These differences were calculated across specific points on individual curves that occurred at slightly different percentages of the gait cycle; ensemble averaging tended to smooth through these true differences, making them less apparent visually. Perhaps more importantly, even with a Bonferroni adjustment, the very powerful dependent *t*-test uncovered systematic differences between models. Inspection of individual curves for sagittal plane hip, knee, and ankle angles suggested that a posterior movement of the lateral knee marker (L/RKNE) in CGM during knee flexion might explain these subtle differences. In fact, such a skin movement

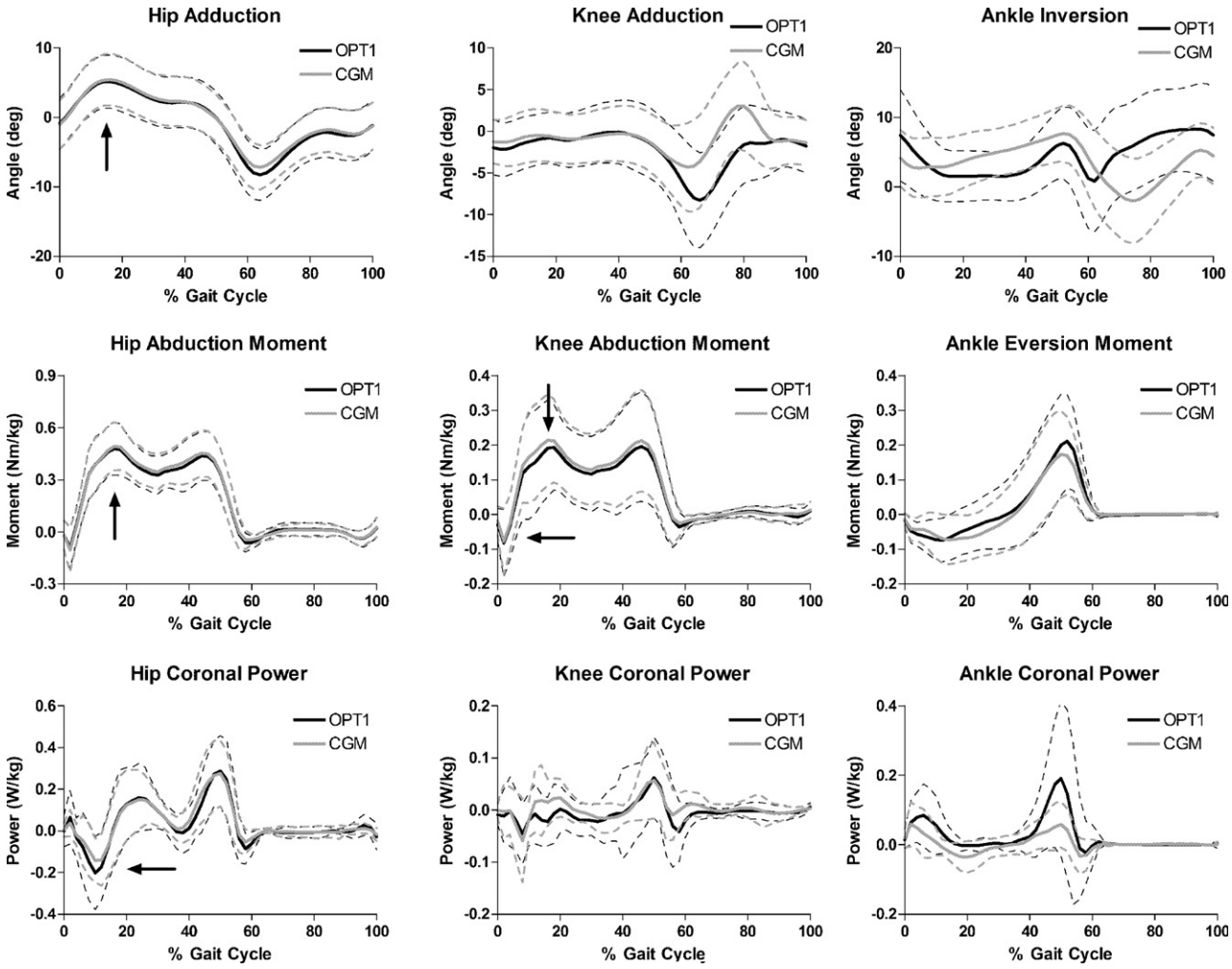

Fig. 3. Coronal plane ensemble averages for 25 normal children. Black arrows indicate where CGM (solid gray) and OPT1 (solid black) were compared statistically with dependent *t*-tests; no statistically significant differences were found ($p < 0.0025$); dashed lines indicate ±one standard deviation.

artifact had been reported by others [16,17], or could be inferred from their results [18], and was demonstrated in skeletal graphics created by Visual3D. By tracking the thigh with a cluster of four markers, OPT1 correctly rendered the femur anterior to the lateral knee marker during flexion; in contrast, CGM used the lateral knee marker to track the thigh, and incorrectly rendered the femoral epicondyle coincident with it. This created a slight shift toward hip and knee extension for CGM. Other sagittal plane differences in ankle angles, moments, and powers were attributed to the more comprehensive, rigid body, foot model in OPT1, rather than the vector approximation in CGM.

Ensemble averages for coronal plane joint angles, moments, and powers (Fig. 3) were generally comparable between CGM and OPT1, and were consistent with somewhat sparse data available in the literature (hip angles, moments, and powers, knee angles and moments, ankle moments [1,13,14]). There were, however a few notable differences. The knee angle at the stance-swing transition (approximately 60% of the gait cycle) was more abducted for OPT1 than for CGM, and a slight adduction peak at early swing was missing for OPT1. These differences were within the variability reported by Kadaba et al. [1, p. 390] for misalignment of the knee LRF of ±5°. The ankle eversion (abduction) moment was nearly identical for OPT1 and CGM, however, an eversion peak at late stance for our data was not present in data reported by Kadaba et al. [13]. Coronal plane differences between OPT1 and CGM for ankle angles and powers were also attributed to the rigid body model used in OPT1. These qualitative observations, as well as the lack of statistically significant differences among coronal plane gait variables (Table 2), suggest that clinical interpretations of these normal data would be unaffected by the choice of CGM or OPT1.

Ensemble averages for transverse plane joint angles, moments, and powers (Fig. 4) were generally comparable between CGM and OPT1, but at times inconsistent with data available in the literature. Our hip angles were consistent with Kadaba et al. [1] and Schache et al. [19] using their Dynamic method, but more externally rotated than Kadaba et al. [13]. In contrast, our knee angles were more externally rotated than Kadaba et al. [1], and consistent with Kadaba et al. [13]. These inconsistencies highlight the importance of avoiding the use of the term "standard" in the context of CGM. Although referencing the identical study, Kadaba et al. [13] used planes formed by the proximal joint, lateral wand, and distal joint to define LRFs in the thigh and shank, while Kadaba et al. [1] applied an additional offset to these LRFs to produce neutral transverse plane rotations during a static calibration. Our hip, knee, and ankle moments were similar in shape, but opposite in sense to those reported by Kadaba et al. [13], i.e., our moments were all biased toward external rotation rather than internal rotation. Such a difference could change the clinical interpretation of these normal data. However, if the moments reported by Kadaba et al. [13] were with respect to the distal rather than proximal segment LRF (as was customary for some researchers at that time), this would explain the differences we found.

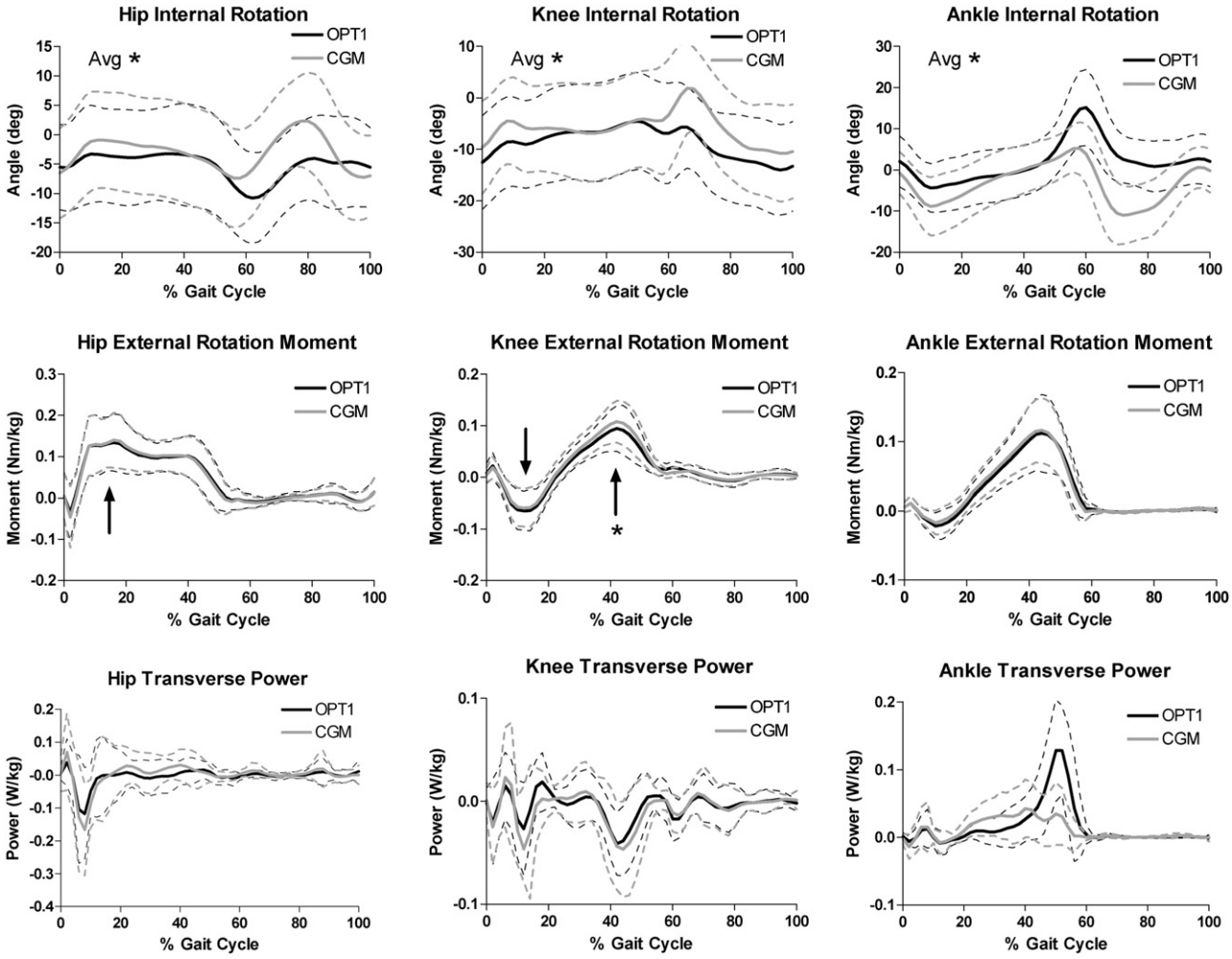

Fig. 4. Transverse plane ensemble averages for 25 normal children. Joint angles averaged across the gait cycle were compared statistically across CGM (solid gray) and OPT1 (solid black) using dependent *t*-tests; black arrows indicate where joint moments were compared; asterisks indicate significant differences ($p < 0.0025$); dashed lines indicate ±one standard deviation.

4.2. Studies free from skin movement artifact

As a preliminary assessment of accuracy, we compared our results to *in vivo* and *in vitro* studies for knee kinematics. Lafortune et al. [20] used bone pins to study *in vivo* tibiofemoral kinematics in five walking adults, providing the closest comparison to the loaded joints analyzed in our study. Differences in sagittal plane knee kinematics were unremarkable. Our knee adduction results, calculated using OPT1, were similar to four of the five subjects in Lafortune et al. [20], and to the reported mean. Our results for CGM were similar to one subject identified by Lafortune and colleagues as an outlier. Our knee internal rotation results, calculated using either CGM or OPT1, were similar in shape to Lafortune et al. [20], but displaced toward external rotation by approximately 5°. This offset is likely due to differences in alignment of the mediolateral axis in the shank LRF. Lafortune et al. [20, p. 348] defined this axis "parallel to a line connecting the centers of the proximal articular surfaces" of the tibia. In contrast, for CGM and OPT1 this axis was parallel to the bi-malleolar axis, and would be more externally rotated due to natural tibial torsion. In an *in vitro* study of 15 cadaveric knees, Wilson et al. [21] found nearly neutral adduction, and internal rotation increasing to approximately 15° as the unloaded knee was flexed to 60°. Similarly, coupled rotations and displacements as a function of knee flexion angle were reported by Walker et al. [22] in an *in vitro* study of 23 cadaveric knees. Their Eqs. (1) and (2) would predict peak adduction (varus) of approximately 2°, and peak internal rotation of approximately13°, as a normal knee was flexed to 60°. Our results did not reflect these intimately coupled motions across the gait cycle, but did reflect *in vivo* data presented by Lafortune et al. [20]. We believe this may be because Walker et al. [22] did not load their specimens in a manner consistent with actual gait. When the knee is loaded, these coupled motions have been shown to disappear [23].

5. Conclusions

Results for all three anatomical planes require more rigorous accuracy tests. In the meantime, our study shows that for normal children, sagittal, coronal, and transverse plane biomechanical interpretations, based upon these tested variables, are unlikely to change due to independent segment tracking alone (CGM vs. OPT1). The value in these methods seems instead to involve higher fidelity input for forward dynamics, and we intend to explore this as one measure of accuracy. These relationships may change when pathological movements exacerbate model differences in a companion study of patients not yet completed. Additional differences may appear if, as planned for our OPT2 model, joint centers and LRFs are changed from those used in CGM, either to reflect new studies [24] or specific abnormal patient anatomy.

Conflict of interest statement

The Motion Analysis Laboratory at Shriners Hospitals for Children, Erie, PA, USA, was a beta test site for Visual3D software for a portion of the time during which this study was conducted.

Disclaimer

The findings and conclusions in this report are those of the authors and do not necessarily represent the views of the National Institute for Occupational Safety and Health.

Acknowledgments

This work was accomplished while the authors were employed at the Motion Analysis Laboratory, Shriners Hospitals for Children, Erie, PA, USA. The authors wish to thank Vineet Sharma, M.S., Stacey L. Gorniak, Ph.D., and Daniel Gloekler, B.S. for their efforts to collect and process walking trials for our 6DoF normal database.

Appendix A. Supplementary data

Supplementary data associated with this article can be found, in the online version, at doi:10.1016/j.gaitpost.2009.08.245.

References

[1] Kadaba MP, Ramakrishnan HK, Wootten ME. Measurement of lower extremity kinematics during level walking. J Orthop Res 1990;8(3):383–92.
[2] Davis RB, Ounpuu S, Tyburski D, Gage JR. A gait analysis data collection and reduction technique. Hum Mov Sci 1991;10:575–87.
[3] Lu TW, O'Conner JJ. Bone position estimation from skin marker co-ordinates using global optimisation with joint constraints. J Biomech 1999;32(2):129–34.
[4] Charlton IW, Tate P, Smyth P, Roren L. Repeatability of an optimised lower body model. Gait Posture 2004;20(2):213–21.
[5] Reinbolt JA, Schutte JF, Fregly BJ, Koh BI, Haftka RT, George AD, Mitchell KH. Determination of patient-specific multi-joint kinematic models through two-level optimization. J Biomech 2005;38(3):621–6.
[6] Buczek FL, Kepple TM, Siegel KL, Stanhope SJ. Translational and rotational joint power terms in a six degree-of-freedom model of the normal ankle complex. J Biomech 1994;27(12):1447–57.
[7] Cappozzo A. Three-dimensional analysis of human walking: experimental methods and associated artifacts. Hum Mov Sci 1991;10:589–602.
[8] Spoor CW, Veldpaus FE. Rigid body motion calculated from spatial co-ordinates of markers. J Biomech 1980;13(4):391–3.
[9] Challis JH. A procedure for determining rigid body transformation parameters. J Biomech 1995;28(6):733–7.
[10] Zajac FE, Gordon ME. Determining muscle's force and action in multi-articular movement. Exerc Sport Sci Rev 1989;17:187–230.
[11] Kuo AD. A least-squares estimation approach to improving the precision of inverse dynamics computations. J Biomech Eng 1998;120(1):148–59.
[12] King HA, Staheli LT. Torsional problems in cerebral palsy. Foot Ankle 1984;4(4):180–4.
[13] Kadaba MP, Ramakrishnan HK, Wooten ME, Gainey J, Gorton G, Cochran GVB. Repeatability of kinematic, kinetic, and electromyographic data in normal adult gait. J Orthop Res 1989;7:849–60.
[14] Ounpuu S, Gage JR, Davis RB. Three-dimensional lower extremity joint kinetics in normal pediatric gait. J Pediatr Orthop 1991;11(3):341–9.
[15] Ounpuu S, Davis RB, DeLuca PA. Joint kinetics: methods, interpretation and treatment decision-making in children with cerebral palsy and myelomeningocele. Gait Posture 1996;4:62–78.
[16] Lafortune MA, Lake MJ. Errors in 3D analysis of human movement. In: Proceedings of the international conference on three-dimensional analysis of human movement; 1991. p. 55–6.
[17] Sati M, de Guise JA, Larouche S, Drouin G. Quantitative assessment of skin-bone movement at the knee. Knee 1996;3:121–38.
[18] Gao B, Zheng N. Investigation of soft tissue movement during level walking: translations and rotations of skin markers. J Biomech 2008;41(15):3189–95.
[19] Schache AG, Baker R, Lamoreux LW. Defining the knee joint flexion-extension axis for purposes of quantitative gait analysis: an evaluation of methods. Gait Posture 2006;24(1):100–9.
[20] Lafortune MA, Cavanagh PR, Sommer HJ, Kalenak A. Three-dimensional kinematics of the human knee during walking. J Biomech 1992;25(4):347–57.
[21] Wilson DR, Feikes JD, Zavatsky AB, O'Connor JJ. The components of passive knee movement are coupled to flexion angle. J Biomech 2000;33(4):465–73.
[22] Walker PS, Rovick JS, Robertson DD. The effects of knee brace hinge design and placement on joint mechanics. J Biomech 1988;21(11):965–74.
[23] MacWilliams BA, Wilson DR, DesJardins JD, Romero J, Chao EY. Hamstrings cocontraction reduces internal rotation, anterior translation, and anterior cruciate ligament load in weight-bearing flexion. J Orthop Res 1999;17(6):817–22.
[24] Bruening DA, Crewe AN, Buczek FL. A simple, anatomically based correction to the conventional ankle joint center. Clin Biomech 2008;23:1299–302.